JACS
JOURNAL OF THE AMERICAN CHEMICAL SOCIETY
Article
pubs.acs.org/JACS

Conformational Analysis of Single Perfluoroalkyl Chains by Single-Molecule Real-Time Transmission Electron Microscopic Imaging

Koji Harano,*[,†] Shinya Takenaga,[†] Satoshi Okada,[†] Yoshiko Niimi,[‡] Naohiko Yoshikai,[†,▽] Hiroyuki Isobe,[†,○] Kazu Suenaga,[§] Hiromichi Kataura,[∥] Masanori Koshino,*[,‡,§] and Eiichi Nakamura*[,†,‡]

[†]Department of Chemistry, The University of Tokyo, Hongo, Bunkyo-ku, Tokyo 113-0033 Japan

[‡]Nakamura Functional Carbon Cluster Project, ERATO, JST, 4-1-8 Honcho Kawaguchi, Saitama, 332-0012 Japan

[§]Nanotube Research Center, National Institute of Advanced Industrial Science and Technology (AIST), Tsukuba, 305-8565 Japan

[∥]Nanosystem Research Institute, National Institute of Advanced Industrial Science and Technology (AIST), Tsukuba, 305-8562 Japan

Supporting Information

ABSTRACT: Whereas a statistical average of molecular ensembles has been the conventional source of information on molecular structures, atomic resolution movies of single organic molecules obtained by single-molecule real-time transmission electron microscopy have recently emerged as a new tool to study the time evolution of the structures of individual molecules. The present work describes a proof-of-principle study of the determination of the conformation of each C−C bond in single perfluoroalkyl fullerene molecules encapsulated in a single-walled carbon nanotube (CNT) as well as those attached to the outer surface of a carbon nanohorn (CNH). Analysis of 82 individual molecules in CNTs under a 120 kV electron beam indicated that 6% of the CF_2−CF_2 bonds and about 20% of the CH_2−CH_2 bonds in the corresponding hydrocarbon analogue are in the gauche conformation. This comparison qualitatively matches the known conformational data based on time- and molecular-average as determined for ensembles. The transmission electron microscopy images also showed that the molecules entered the CNTs predominantly in one orientation. The molecules attached on a CNH surface moved more freely and exhibited more diverse conformation than those in a CNT, suggesting the potential applicability of this method for the determination of the dynamic shape of flexible molecules and of detailed conformations. We observed little sign of any decomposition of the specimen molecules, at least up to 10^7 e·nm^{-2} (electrons/nm^2) at 120 kV acceleration voltage. Decomposition of CNHs under irradiation with a 300 kV electron beam was suppressed by cooling to 77 K, suggesting that the decomposition is a chemical process. Several lines of evidence suggest that the graphitic substrate and the attached molecules are very cold.

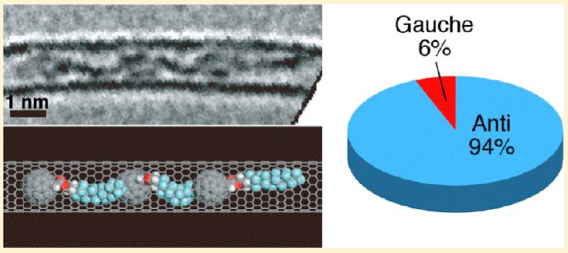

INTRODUCTION

In an ensemble of molecules of a complex compound, transitions between conformational states depend on the energy barriers between them. Thus, a molecule (gray) in conformation B can rapidly equilibrate, thermally, to the next conformation A or C, whereas another molecule (white) in conformation D is likely to remain there for a long time because of the high energy barrier that separates the minima C and D (Figure 1). Organic chemists, when planning their experiments, often carry out such a molecule-by-molecule analysis of conformation on a molecular model to consider the effects of the local conformation and of the overall shape of the molecule. However, to date, there has been no experimental method that directly supports such an intuitive approach of conformational analysis that tells us which C−C bond in a molecule takes what conformation, how often, and what kind of overall shape is preferred among the many possibilities. This is largely because the major source of our conformational knowledge relies on the measurement of time- and molecular-average of ensembles as demonstrated by spectroscopic and crystallographic analyses.[1,2]

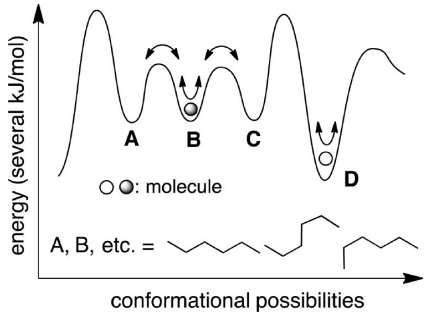

Figure 1. Two hydrocarbon molecules (gray and white) equilibrating on a conformational potential surface.

Received: November 3, 2013
Published: December 17, 2013

   dx.doi.org/10.1021/ja411235x | J. Am. Chem. Soc. 2014, 136, 466−473

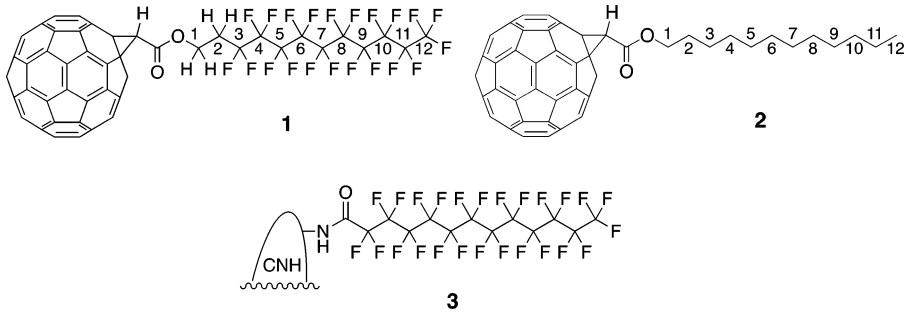

Figure 2. Structures of the perfluoroalkyl fullerene **1**, alkyl fullerene **2**, and perfluoroalkyl carbon nanohorn **3**.

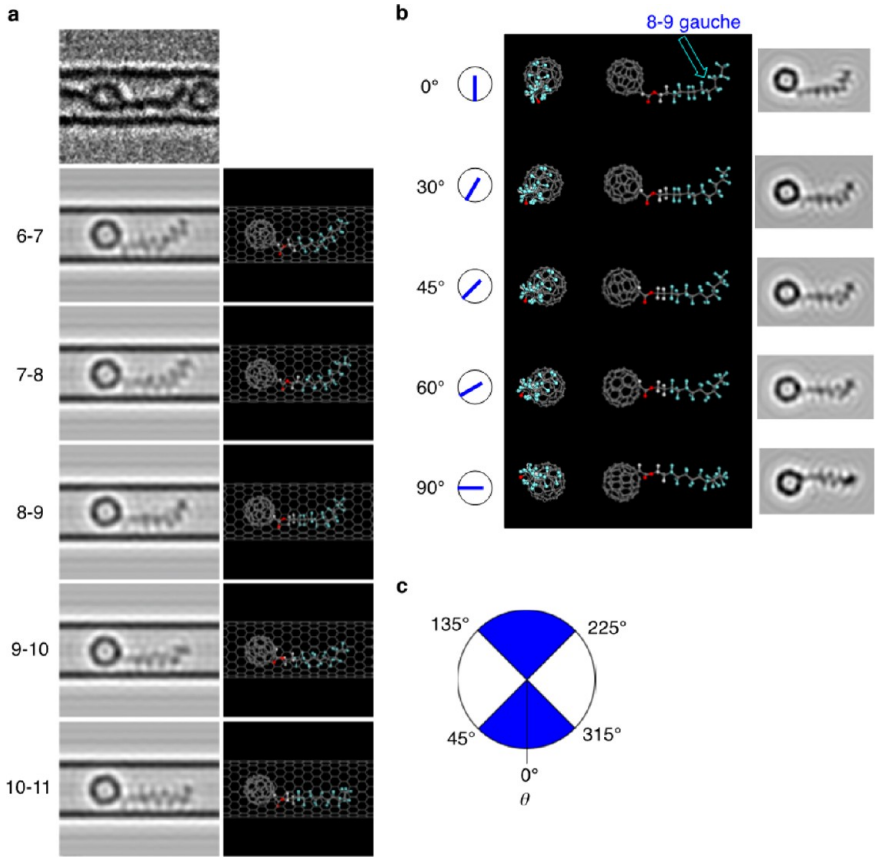

Figure 3. Various views of molecular models and their TEM simulation of molecule **1** in which the C8−C9 bond is gauche, and simulated TEM images of **1** with one gauche conformation in different positions. The angle θ is defined in the left column, where $\theta = 0°$ indicates that C8−C9−C10 atoms are in the plane of the paper. (a) Simulated TEM images of **1** with one gauche conformation in different positions and an image of the real molecule on the top that has a gauche C8−C9 bond. (b) Views of C8−C9 gauche conformer from various angles, and (c) quadrants of the angle θ in blue, where accurate structural determination is possible.

We have expended considerable effort over a long time,[3,4] to study the structure of single molecules[5] and molecular clusters[6] and their evolution over time (conformation, reaction[7] and catalysis[8]), by recording movies of molecules and molecular clusters in vacuum by atomic resolution transmission electron microscopy (TEM), as illustrated by a real-time movie of two wobbling hydrocarbon chains in a single molecule located in a carbon nanotube (CNT), first reported in 2007.[9] The images in this single-molecule real-time TEM (SMRT-TEM) movie were often blurred because the motion was faster than the speed of the image acquisition on the charge-coupled device (CCD) camera (0.5 s). There are two conceivable solutions, namely, the use of a less mobile specimen or of a faster CMOS camera with an imaging speed of <1 ms. In this study, we elected to use the first option; the latter is not yet available on the market.[10]

The selected proof-of-principle specimen molecule was a perfluoroalkyl (PF = $C_{10}F_{21}$) chain attached to a fullerene core (**1**) encapsulated in a CNT. The CF_2−CF_2 bond is conformationally much less flexible than a CH_2−CH_2 bond, preferring an all-anti conformation (Figure 2).[11] A hydrocarbon analogue **2** was also studied as a reference standard (Figure 2).

We report here that 18 of the 19 tadpole-shaped molecules **1** that we studied in detail maintained one conformation and one molecule took two conformations, as observed during TEM observation over a period of a few minutes, and that the 20 conformers of **1** allowed us to determine the anti/gauche ratio of all CF_2−CF_2 bonds in each conformer. The probability of

dx.doi.org/10.1021/ja411235x | J. Am. Chem. Soc. 2014, 136, 466−473

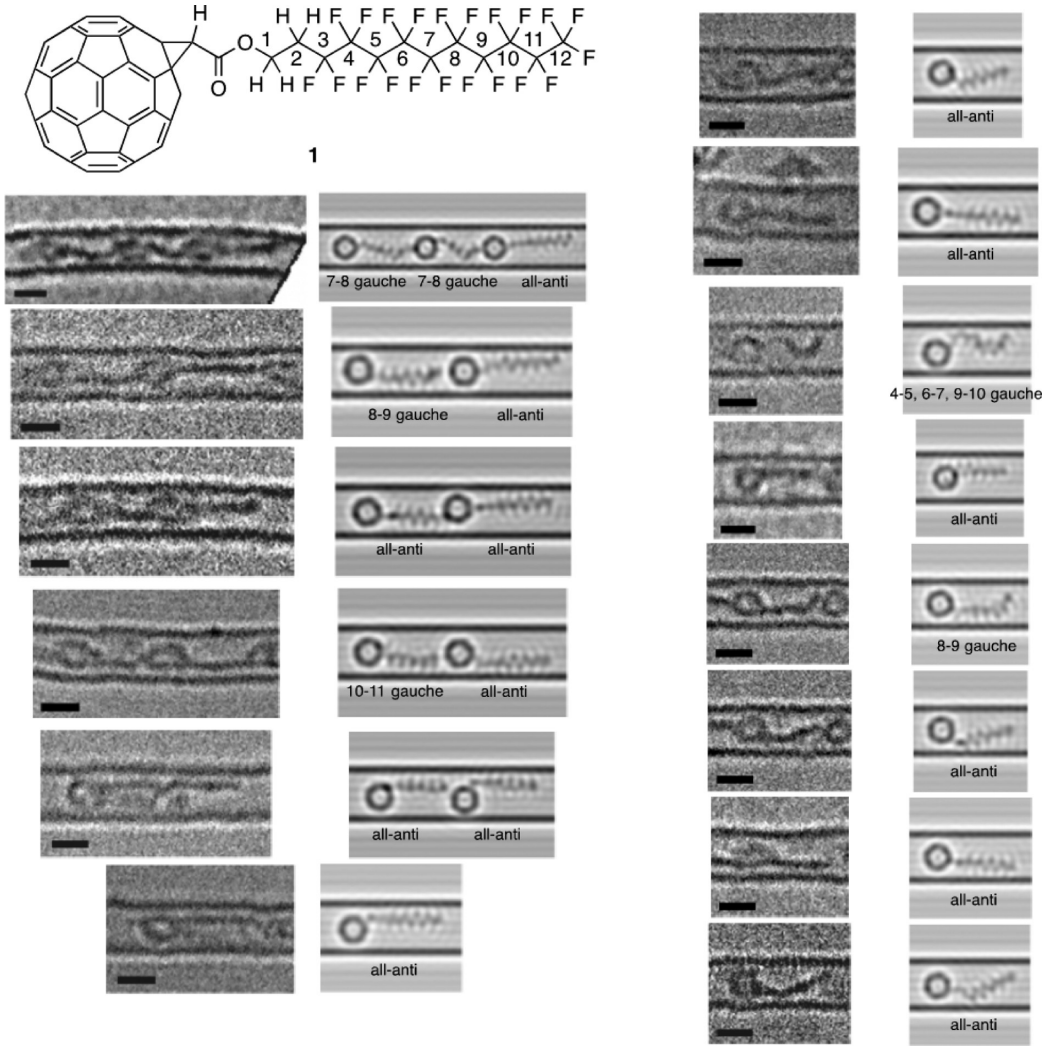

Figure 4. TEM images of 20 PF fullerene molecules **1** and their simulation. Locations of the gauche C−C bonds are indicated below each simulation. The white lines parallel to the dark lines of the CNT walls are Fresnel interference fringes, which may have distorted the molecular images. Translation of the molecules during observation may also be a reason for the blurred images of fullerene and other parts of the molecules. Scale bar is 1 nm.

any CF_2−CF_2 bond being in the gauche conformation was the same for each, at about 6%. The CH_2−CH_2 bonds in **2** are several times more frequently found in the gauche conformation than the CF_2−CF_2 bonds are. This marked preference of the anti configuration of the CF_2−CF_2 bonds is in agreement with the ensemble average data, spectroscopic data on perfluorobutane and crystal structures of long perfluoroalkyl chains.[11]

We also studied the behavior of perfluoroalkyl chains attached on the outer surface of a tapered variant of a CNT, called a carbon nanohorn (CNH, **3**), and found that they are as stable as **1** and **2** in CNTs against electron irradiation. The molecules of **3** can, as expected, take a wider variety of conformations, but their motions were found to be quite slow and very restricted by the weak CF−π van der Waals interactions with the surface of the CNH. Imaging of CNHs at different acceleration voltages, total electron doses, and temperatures indicated that CNH decomposition is strongly temperature dependent.

RESULTS AND DISCUSSION

Compounds **1** and **2** were synthesized by esterification of a known [60]fullerene carboxylic acid.[12] The fullerene moiety in these molecules acts as an anchor that guides the molecule into an oxidatively perforated CNT (diameter 1.4 ± 0.1 nm) through fullerene/CNT π−π interaction, and the CH_2CH_2OCO group in **1** acts as a flexible linker that allows the PF moiety to take an energetically relaxed shape in the narrow space in the CNT. We also studied a perfluoroalkyl ($C_{12}F_{25}$) amide attached to the surface of a CNT (**3**) as a reference molecule exposed in vacuum. For this purpose, we used CNHs bearing amino groups, which we acylated with $C_{12}F_{25}COCl$ to obtain **3**.[13]

TEM imaging of specimens was typically carried at 293 K at an acceleration voltage of 120 kV, except for some experiments that were carried out at 77 K and 60−300-kV acceleration voltages (as indicated). The imaging was carried out for several minutes, up to a total electron dose of ca. 1×10^7 e·nm^{-2} (electrons/nm^2).

Determination of the Conformation of the PF Chain of 1. We first describe the method for determination of the

dx.doi.org/10.1021/ja411235x | J. Am. Chem. Soc. 2014, 136, 466−473

conformation of **1** through the analysis of each frame of the molecular movies. Our ability to obtain pseudo-three-dimensional information of the molecule was essential for structure determination; that is, the molecules spontaneously rotated during movie recording so that we could view each single molecule from different directions (as we do in a theatrical movie or on television).

We first describe an example of the structural identification of a C8−C9 gauche conformer of **1**, whose experimental TEM image is shown in Figure 3a (top), followed by simulated TEM and molecular images of the molecules, one of whose C*n*−C*n*+1 bonds is gauche for n = 6−10. This experimental TEM image is so clear that we can assume that the C8−C9 bond is in gauche conformation, even without recourse to the use of any reference TEM images.

Since the molecules spontaneously rotate in the CNT along the CNT axis, we sometimes see them in the best orientation, as in Figure 3a, but often in a much less suitable orientation against the electron beam. Therefore, we needed to calibrate our ability of determine the anti/gauche conformation of the molecules that are not ideally disposed. Thus, we created a series of TEM simulations of a model of **1** by rotating the molecule through various angles θ (an angle between the electron beam and the C8−C9−C10 atoms in the plane of the paper). We varied θ from 0° to 90°, with a step of 15−30°, and show the molecules with their C8−C9−C10 atoms in the plane of the paper, with C10 pointing toward the viewer (Figure 3b). Between θ = 0° and 45°, we can easily identify the position of the gauche bond, but not for θ > 60°, as expected. Thus, we can assign the structure of **1** if θ remains in the blue quadrants shown in Figure 3c. In this way, we can determine the position of a gauche bond in **1** with an accuracy of less than ±1 bond.

It should be noted that the anti CF_2−CF_2 chain is known to be helical to some extent.[14] We could however not address such a subtle issue because of the low resolution of the presently available TEM instrumentation. Furthermore, because of the increased conformational possibilities, we could assign the conformation of **2** with much less accuracy than **1**. Future developments in TEM instrumentation should offer us better time and space resolution in the near future.

In the manner described above, we could determine the conformation of 19 clearly discernible, rotating molecules of **1** chosen from 82 molecules that we could analyze in some detail (details of the procedure and larger pictures are given in the Supporting Information). During the observation period of half a minute to a few minutes, one specimen changed one gauche C−C bond to anti. This allowed us to observe an additional conformer of the same molecule, and we counted both separately in the distribution analysis, increasing the total number of specimens to 20. (All images are shown in Figure 4.)

A similar conformational analysis was performed for 20 specimens of molecule **2**. Here we analyzed the conformation with lower accuracy because of the larger flexibility and the less dense images because of the smaller atomic number of hydrogen in the alkyl chain than fluorine in the PF chain (through comparison with TEM simulations shown in the Supporting Information).

Summary of Conformation of 1 and 2. A summary of the anti/gauche conformational property of **1** is shown in Figure 5a and c. Figure 5a summarizes a total of 140 data for the 7 CF_2−CF_2 bonds in each molecule of **1** for 20 conformers. Thus, 8 (6%) are gauche and 132 are anti (94%). Figure 5a also shows that any one of the C−C bonds may be in gauche

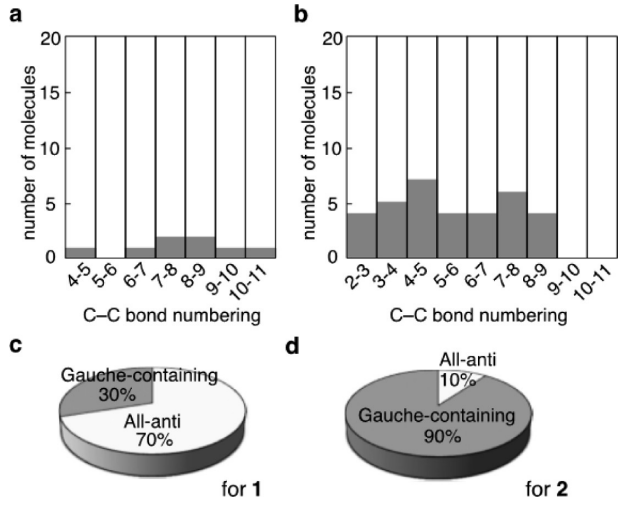

Figure 5. Summary of the conformational behavior of **1** and **2**. (a, b) Anti/gauche ratio of individual C−C bonds in (a) the PF chain of **1** and (b) the alkyl chain of **2**. (c, d) Ratio of all-anti and gauche-containing molecules for (c) **1** and (d) **2** in a CNT.

conformation in a probability of 0−10%. Figure 5c indicates the ratio of all-anti conformer vs conformers having at least one gauche to be 70:30. This type of information is hardly obtainable by any other known analytical methods, and therefore illustrates the unusual potential of the SMRT-TEM method in structural analysis.

The flexibility and the low TEM contrast of **2** did not permit us to obtain data as accurately as we did for **1**. Nonetheless, we summarize the data in Figure 5b, which indicates that, among the total of 180 CH_2−CH_2 bonds studied, 34 (19%) are gauche and 146 (81%) anti. Figure 5d indicates the ratio of all-anti conformer vs conformers having at least one gauche to be roughly 10:90.

Imaging of a PF Chain on the Outside of CNH. A PF chain **3** attached on the surface of a CNH provided information on three important issues: the stability of the PF groups against an electron beam, the conformational mobility of the PF chain without CNT encapsulation, and the extremely slow (order of seconds) conformational change indicating that the molecule is extremely cold. As illustrated by two frames of a movie taken during 126 s with a 120 kV electron beam in Figure 6a (two specimens indicated by red arrows), the two PF chains remained stable up to the total dose of 1.4×10^7 e·nm^{-2}. If the C−C and C−N bonds in **3** were broken by electron impact, or for any other reason, the image of the PF chain would have been lost. Examination of 25 specimen molecules in nine movies revealed all molecule surfaces with electron irradiation up to 3.6×10^7 e·nm^{-2} at 120 kV, except one, the whole part of which was lost at a dose of 2.0×10^7 e·nm^{-2}. The loss of the whole part, instead of only a part, suggests the cleavage of the CNH−amide bond rather than the C−C bond of the PF chain or decomposition of the CNH substrate (see the Supporting Information). This stability of isolated PF molecules up to 2×10^7 e·nm^{-2} stands in sharp contrast to the instability of the PF fullerene **1** in a solid state, which started to decompose at a dose as small as 4.0×10^5 e·nm^{-2} as revealed by electron energy loss spectroscopy (EELS) analysis conducted at 120 kV (Figure 7 and Figure S5 in the Supporting Information). This instability of the solid **1** is just as unstable as other organic solid under TEM conditions,[15] where the electrons irradiated on

dx.doi.org/10.1021/ja411235x | J. Am. Chem. Soc. 2014, 136, 466−473

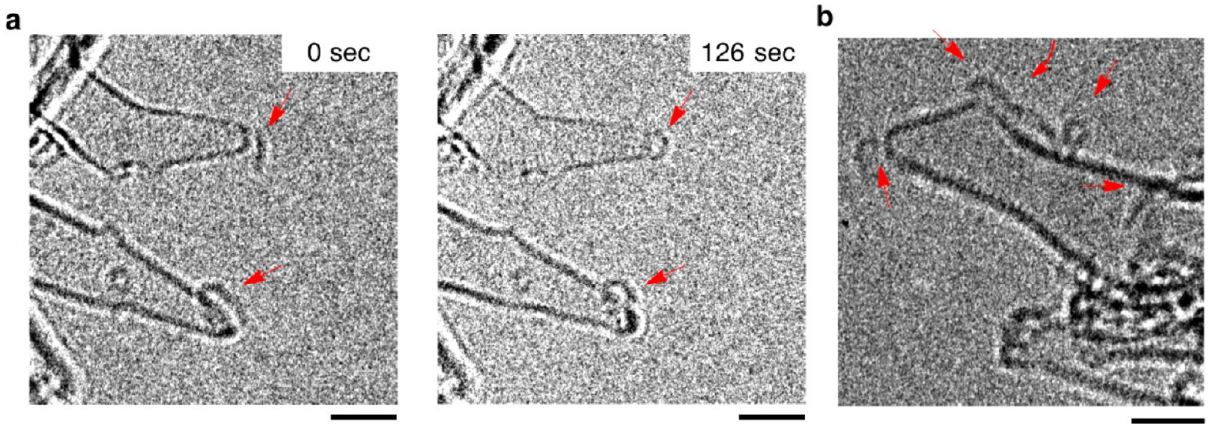

Figure 6. TEM observation of PF−CNH **3** at 293 K. (a) TEM images taken at 120 kV. The inset refers to the time (seconds) after initiation of the observation, that is, initiation of electron irradiation. The total electron dose during the 126 s observation is 1.4×10^7 e·nm^{-2}. (b) Image taken at 60 kV. Arrows indicate the $C_{12}F_{25}$ chain. Scale bars are 2 nm.

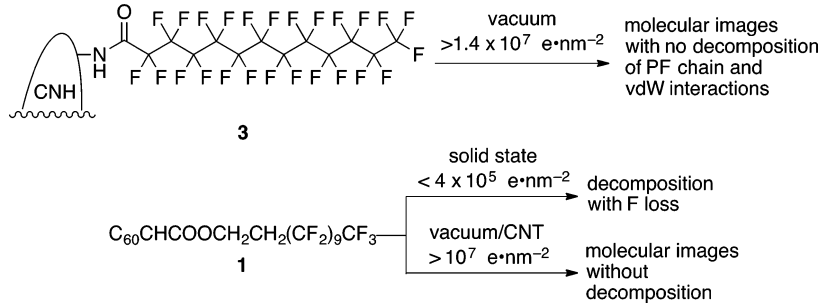

Figure 7. Stability of **1** and **3** under SMRT-TEM conditions and instability of **1** in solid state.

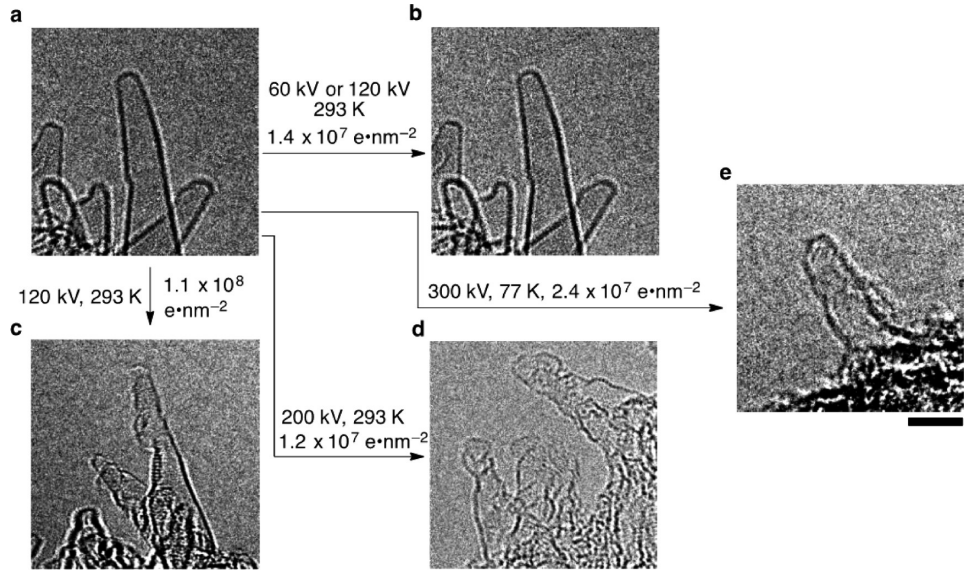

Figure 8. Stability of carbon nanohorns under different TEM conditions. Images of the same nanohorns (a) before and (b) after irradiation of 10^7 e·nm^{-2} electrons at 60 kV. (c−e) Images of nanohorns recorded in separate experiments, showing bulging formations. Scale bar is 3 nm.

organic solid cause crystalline lattice disorder, a cascade of collisions with molecules (scattered electrons and secondary electrons) and intermolecular radical reactions among closely packed molecules. Under the SMRT-TEM conditions, the collision between an electron and a single molecule occurs only once and does not cause the cascade of collisions and no intermolecular reactions occur even though there may form a radical species.

We see that the molecule in the top in Figure 6a at 0 s is linear and the one at 126 s is bent. The bent conformation was found in the molecule in the bottom of Figure 6a and b (and widely seen for other molecules not shown), caused by van der Waals interaction with the CNH surface. It is remarkable that even such an extremely weak CF−π interaction (e.g., CF_4−benzene interaction energy of 3.6 kJ/mol)[16] was maintained under the TEM conditions, which indicates that the molecules

dx.doi.org/10.1021/ja411235x | J. Am. Chem. Soc. 2014, 136, 466−473

are extremely cold (i.e., small vibrational energy) even though the sample stage is at 293 K. At the 120-kV acceleration voltage, we often saw the molecular images blurred due to rapid motion of the PF chain during the irradiation period of 0.5 s, but very seldom at a 60-kV acceleration voltage (Figure 7b), suggesting that the system is even more colder than the one at 120 kV. The frequent blurring of **3** at 120 kV stands in contrast to the very infrequent blurring of a biotin triamide similarly attached on the surface of a CNH and observed at 120 kV electron beam.[17] This must be due to the much stronger van der Waals interaction between the biotin triamide and the π-electron rich surface of the CNH compared with the CF–π interaction between **3** and CNH.

Decomposition of a CNH at Various Acceleration Voltages and Temperatures. We next describe how the instability of the CNH substrates can be suppressed by reducing the reaction temperature and the acceleration voltage (Figure 8).[18] Thus, the CNHs on a specimen stage at 293 K showed little sign of decomposition at 60 kV or 120 kV with a total electron dose in the order of 10^7 e·nm^{-2} (the conditions where **1**–**3** showed little sign of decomposition) (Figure 8b), but decomposed extensively with a total dose of 10^8 e·nm^{-2} at 120 kV (Figure 8c). Therefore, there was a threshold of CNH decomposition around 5×10^7 e·nm^{-2} at 120 kV. A 200-kV electron dose caused significant damage already in the range of 10^7 e·nm^{-2} (Figure 8d). Then, we found that the decomposition could be effectively suppressed at 77 K even at 300 kV (Figure 8e; during imaging for 5 min with up to 2.4×10^7 e·nm^{-2}) (see the Supporting Information). Such a large temperature dependence is characteristic of chemical reactions rather than of atom-by-atom knock-on damage by the electron beam that is known to be a temperature-independent event.[19]

One standard method to characterize the nature of chemical reactions is the $^{12}C/^{13}C$ primary kinetic isotope effect (KIE). This value is generally no greater than 1.1 above 200 K for C–X bond cleavage (X = H, C, or heteroatom), but can increase precipitously as the temperature becomes closer to 0 K (Figure 9), because, at low temperature, the zero-point energy (ZPE) term dominates over two other terms, mass moment of inertia and excitation factor. Therefore, one can estimate the KIE value for homolytic cleavage of $H_2C{=}CH_2$ to increase from 1.16 at 300 K, 2.50 at 50 K, to 6.22 at 25 K based on ZPE difference of ^{12}C- and ^{13}C-ethylene molecules (ca. 0.38 kJ mol^{-1}; calculated from C=C stretching frequencies of 1600 and 1540 cm^{-1} for ^{12}C and ^{13}C, respectively; Figure 9). Simultaneous homolytic cleavage of three C–C bonds around one carbon atom in a graphene sheet can cause even greater KIE at low temperatures. Thus, simply by triplicating the ZPE difference of ethylene, KIE can be roughly estimated to be 1.58 at 300 K, 15.5 at 50 K, and 241 at 25 K. The experimental $^{12}C/^{13}C$ KIE value reported for the zeroth-order loss of carbon atoms from a graphene sheet under TEM conditions was 5.5–6.5.[18] Such a large value indicates that the graphene skeleton is extremely cold, say 25 K (i.e., small vibrational energy), which we also found for the slow motions of the PF molecule on CNH. This value of 5.5–6.5 suggests that only one C–C bond is cleaved at a rate determining step of a multistep mechanism of the carbon atom loss, instead of one-step loss of a carbon from graphene, CNT and CNH (Figure 9). The very large KIE indicates that ^{13}C-graphitic substrates are more stable and hence more suitable for SMRT-TEM imaging.

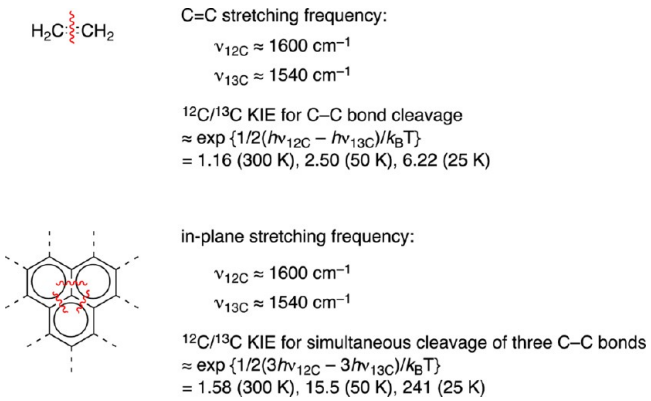

Figure 9. Estimated primary $^{12}C/^{13}C$ KIE values for C=C bond cleavage of ethylene and graphene (one step loss of a carbon atom via cleavage of three C–C bonds indicated by red wavy lines).

Orientation of Single Molecules of 1 in a CNT. As illustrated in Figure 10 (and Figure S1 in the Supporting Information), the molecules **1** and **2** are encapsulated in an ordered manner. We examined the 82 molecules of **1**, in which the relative orientations of 55 molecules (32 pairs) were clearly identified by comparison with the TEM simulation (see below). For the other 27 molecules, we could not determine the orientation because of the unclear image of the connection between the fullerene and the PF tail. Out of the 32 pairs of molecules, 27 were arranged in a head-to-tail manner (Figure 10a and in the Supporting Information), while one pair of molecules was arranged in a head-to-head manner and four in a tail-to-tail manner. Thus, the head-to-tail vs head-to-head vs tail-to-tail ratio was 84:3:13. We can consider a priori that the molecules **1** and **2** enter the CNT from the fullerene side because of the stronger interaction of CNTs with fullerene than with the PF and the alkyl chains.[20–22]

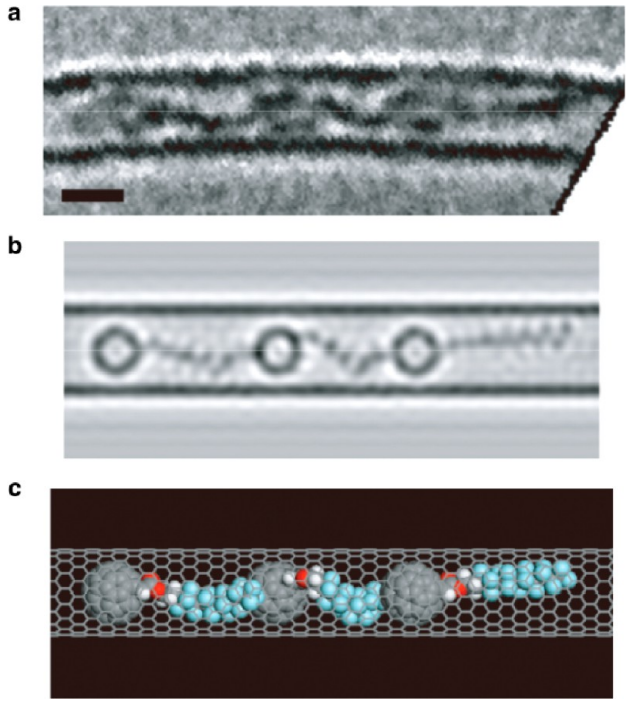

Figure 10. Example of head-to-tail orientation of molecule **1**. (a) TEM image, (b) simulation, and (c) molecular model. Scale bar is 1 nm.

dx.doi.org/10.1021/ja411235x | J. Am. Chem. Soc. 2014, 136, 466–473

CONCLUSION

The high-resolution TEM images of molecules **1** and **2** encapsulated in CNTs and **3** attached on a CNH have shown that SMRT-TEM imaging can provide an intriguing data set to reveal the time-dependent conformational changes of small organic molecules. This is directly relevant to chemists' intuitive comprehension of molecular conformation. Thus, we could visually determine the anti/gauche ratio of all C−C bonds in each molecule of **1** and study the overall shape of the moving molecules. Such information is hardly obtainable by any conventional experimental methods, including scanning probe microscopy analysis of single molecules attached to a flat substrate.[23] The conformational restriction imposed by the CNT encapsulation can be removed by the exterior attachment of a molecule (i.e., **3**). We expect that the experimental protocol reported here will serve as a standard model for future study of the static and dynamic behaviors of organic molecules, using the SMRT-TEM imaging method.

We have also provided a set of experimental data that prove the mildness of the SMRT-TEM imaging of single organic molecules attached to a CNT or CNH. First, the energy given to the PF molecule **3** by the electron beam is just sufficient to disturb the very weak van der Waals interaction[6] between a graphitic carbon surface and the PF chain. This observation coupled with the conformational change taking place in the order of second indicates that the molecule is extremely cold. An extremely large $^{12}C/^{13}C$ KIE reported for decomposition of graphene is also consistent with this behavior of the PF molecule, indicating that the molecules attached to the graphitic material are very cold (for instance at 25 K) even though they are placed on a TEM sample holder at room temperature. Second, TEM imaging does not cleave the C−C and C−N bonds of **3**, and **3** gives more distinct contrast than for hydrocarbons due to the larger atomic number of fluorine than hydrogen. The stability and the high contrast of PF chains are advantageous as markers for structure assignment in SMRT-TEM imaging, as in the case of carboranes, fullerenes and bromine atoms,[6] Third, the comparison of the stability of a single molecule of **1** in vacuum with the same molecule in the solid state was performed for the first time, and it was proved that the a single molecule in vacuum survives under >100 times higher total electron dose than the molecule in solid and CNT/CNH materials (Figure 7); that is, single isolated organic molecules under TEM conditions are stable, whereas organic solid is severely damaged. This is due to the lack of the adverse effects of the cascade of electron scattering for single molecules in vacuum. Finally, the high sensitivity of the CNH decomposition to temperature suggests that the decomposition of graphitic carbon materials is mainly caused by chemical reactions rather than by displacement of each carbon atom by the knock-on effects of electron impact which is insensitive to temperature. The $^{12}C/^{13}C$ KIE analysis indicates that CNH and CNT composed entirely of ^{13}C is more resistant to radiation damage at low temperature and hence more suitable substrate of SMRT-TEM imaging than the ^{12}C counterpart.

EXPERIMENTAL SECTION

Encapsulation of Specimen Molecules to CNTs. A purified sample of CNTs (heating, acid treatment, H_2O_2 treatment, and toluene washing[24]) was used. The average diameter of the CNTs (by TEM analysis) was 1.4 ± 0.1 nm. To remove the end-caps of the CNTs, they were heated (1.0 K/min) under an oxygen gas flow (20 mL/min) in vacuum (~10^2 Pa) and held at 420 °C for 25 min. The open-ended CNTs were heated at 300 °C for 5 h before the encapsulation to avoid encapsulation of water.[25] Specimen molecules (perfluoroalkylfullerene **1** or alkylfullerene **2**) were introduced as follows: a mixture of oxidized CNTs and guest molecules (**1** or **2**) was stirred in toluene at 353 K for 8 h. The mixture was washed with toluene several times, with the intention of removing excess guest molecules. The sample was washed with methanol under sonication for 20 s. The suspension was dropped onto a lacey carbon film precoated on a molybdenum grid disk, which was then heated at 573 K in vacuum (6.0×10^{-4} Pa) for several hours in an attempt to remove solvent and other contaminants. The disk was cooled to 293 K and introduced to the TEM column for observation.

TEM Observation. TEM observations of **1** and **2** at 293 K (120 kV) were carried out using a JEM-2100F instrument (JEOL Ltd.) with a spherical aberration coefficient (Cs) = 0.45 mm at an acceleration voltage of 120 kV under a vacuum of 1.0×10^{-5} Pa in the sample column. A series of TEM images was obtained at time intervals of 2.1 s, with an electron irradiation time of 0.5 s ($0.6\ C{\cdot}cm^{-2} = 3.7 \times 10^4\ e{\cdot}nm^{-2}$), followed by an image readout time of 1.6 s without irradiation. The imaging instruments were either a multiscan camera (1024 × 1024 pixels) or an ultrascan camera (2024 × 2024 pixels). The minimum dose system enabled us to acquire an image without significant electron irradiation before starting the imaging. When the molecules moved during the 0.5 s exposure time, the molecular image became blurred. When the molecules did not move for several seconds, we could superimpose a few images to improve the signal/noise ratio. We noted that the 0.5 and 1.6 s periods are extremely long time scales for vibrations of free-standing molecules, where the time scale of the conformation change is far less than 1 μs.

TEM observations of carbon nanohorns at 293 K (60, 120, and 200 kV) were carried out using a JEM-ARM200F (JEOL Ltd.) instrument with a spherical aberration corrector for objective lens under a vacuum of 1.0×10^{-5} Pa in the sample column. A series of TEM images was obtained at time intervals of 2.1 s with an electron irradiation time of 0.5 s ($2.2 \times 10^5\ e{\cdot}nm^{-2}$ for 60 kV, $1.8 \times 10^5\ e{\cdot}nm^{-2}$ for 120 kV) followed by an image readout time of 1.6 s without irradiation. The imaging instruments were an ultrascan camera (Gatan Co., 2024 × 2024 pixels).

TEM observations of carbon nanohorns at 77 K (300 kV) were taken on a Titan Krios instrument (FEI Company) equipped with autoloader and 4096 × 4096 Falcon II electron detector. A series of TEM images was obtained at time intervals of 1.14 s with an electron irradiation time of 1.0 s ($2.0 \times 10^3\ e{\cdot}nm^{-2}$ per frame) followed by an image readout time of 0.14 s without irradiation.

Simulation of TEM Images. Molecular structures were optimized by molecular mechanics calculations using an OPLS 2005 force field implemented in the MacroModel software.[26] Further optimization of the dihedral angles was performed using Materials Studio[27] to achieve the best fitting of the simulated TEM images and the experimental TEM images. The TEM simulation was performed with software provided by Earl J. Kirkland.[28] Typical parameters for the TEM simulation were E = 120 kV, Cs = 0.45 mm, defocus = −47.5 nm, objective aperture size = 30 mrad, illumination semiangle = 2 mrad, and defocus spread = 3 nm.

ASSOCIATED CONTENT

Supporting Information

Experimental procedures, additional TEM images, TEM movies, and EELS analysis of the PF fullerene in solid state. This material is available free of charge via the Internet at http://pubs.acs.org.

AUTHOR INFORMATION

Corresponding Authors

harano@chem.s.u-tokyo.ac.jp
m-koshino@aist.go.jp
nakamura@chem.s.u-tokyo.ac.jp

Present Addresses

[▽]Division of Chemistry and Biological Chemistry, School of Physical and Mathematical Sciences, Nanyang Technological University, 21 Nanyang Link, 637371 Singapore

[○]Department of Chemistry, Tohoku University, Aoba-ku, Sendai, 980-8578 Japan

Notes

The authors declare no competing financial interest.

■ ACKNOWLEDGMENTS

We thank Mr. Akira Yasuhara (JEOL Ltd.) and Dr. Akihito Kumamoto (The University of Tokyo) for TEM measurement of PF−CNH, and Dr. Matthijn Vos (FEI Company) for TEM measurements at 77 K. This work was partly supported by KAKENHI on Specially Promoted Research (22000008) to E.N., and Innovative Areas "Coordination Programming" (Area 2107, 24108710) to K.H. from MEXT, Japan. Some TEM measurements were conducted in the Research Hub for Advanced Nano Characterization, The University of Tokyo, and supported by "Nanotechnology Platform" (12024046), both sponsored by MEXT, Japan. We thank Dr. Niclas Solin for experimental contributions.

■ REFERENCES

(1) Mizushima, S.; Morino, Y.; Takeda, M. *J. Chem. Phys.* **1941**, *9*, 826.

(2) Karplus, M. *J. Chem. Phys.* **1959**, *30*, 11−15.

(3) Nakamura, E. Carbon Nanotube for Imaging of Single Molecules in Motion. In *Chemistry of Nanocarbons*; Akasaka, T., Wudl, F., Nagase, S., Eds.; Wiley-VCH: Weinheim, 2010; pp 405−412.

(4) Nakamura, E. *Angew. Chem., Int. Ed.* **2013**, *52*, 236−252.

(5) Koshino, M.; Solin, N.; Tanaka, T.; Isobe, H.; Nakamura, E. *Nat. Nanotechnol.* **2008**, *3*, 595−597.

(6) Harano, K.; Homma, T.; Niimi, Y.; Koshino, M.; Suenaga, K.; Leibler, L.; Nakamura, E. *Nat. Mater.* **2012**, *11*, 877−881.

(7) Koshino, M.; Niimi, Y.; Nakamura, E.; Kataura, H.; Okazaki, T.; Suenaga, K.; Iijima, S. *Nat. Chem.* **2010**, *2*, 82−83.

(8) Nakamura, E.; Koshino, M.; Saito, T.; Niimi, Y.; Suenaga, K.; Matsuo, Y. *J. Am. Chem. Soc.* **2011**, *133*, 14151−14153.

(9) Koshino, M.; Tanaka, T.; Solin, N.; Suenaga, K.; Isobe, H.; Nakamura, E. *Science* **2007**, *316*, 853.

(10) Li, X.; Mooney, P.; Zheng, S.; Booth, C. R.; Braunfeld, M. B.; Gubbens, S.; Agard, D. A.; Cheng, Y. *Nat. Methods* **2013**, *10*, 584−590.

(11) Kirsch, P. *Modern Fluoroorganic Chemistry*; Wiley-VCH: Weinheim, 2004.

(12) Tada, T.; Ishida, Y.; Saigo, K. *J. Org. Chem.* **2006**, *71*, 1633−1639.

(13) Isobe, H.; Tanaka, T.; Maeda, R.; Noiri, E.; Solin, N.; Yudasaka, M.; Iijima, S.; Nakamura, E. *Angew. Chem., Int. Ed.* **2006**, *45*, 6676−6680.

(14) Monde, K.; Miura, N.; Hashimoto, M.; Taniguchi, T.; Inabe, T. *J. Am. Chem. Soc.* **2006**, *128*, 6000−6001.

(15) Egerton, R. F.; Li, P.; Malac, M. *Micron* **2004**, *35*, 399−409.

(16) Kawahara, S.-I.; Tsuzuki, S.; Uchimaru, T. *J. Phys. Chem. A* **2004**, *108*, 6744−6749.

(17) Nakamura, E.; Koshino, M.; Tanaka, T.; Niimi, Y.; Harano, K.; Nakamura, Y.; Isobe, H. *J. Am. Chem. Soc.* **2008**, *130*, 7808−7809.

(18) Meyer, J. C.; Eder, F.; Kurasch, S.; Skakalova, V.; Kotakoski, J.; Park, H. J.; Roth, S.; Chuvilin, A.; Eyhusen, S.; Benner, G.; Krasheninnikov, A. V.; Kaiser, U. *Phys. Rev. Lett.* **2012**, *108*, 196102.

(19) Smith, B. W.; Luzzi, D. E. *J. Appl. Phys.* **2001**, *90*, 3509−3515.

(20) Kuwahara, R.; Kudo, Y.; Morisato, T.; Ohno, K. *J. Phys. Chem. A* **2011**, *115*, 5147−5156.

(21) Baowan, D.; Thamwattana, N.; Hill, J. M. *Phys. Rev. B* **2007**, *76*, 155411.

(22) Ulbricht, H.; Moos, G.; Hertel, T. *Phys. Rev. Lett.* **2003**, *90*, 095501.

(23) de Oteyza, D. G.; Gorman, P.; Chen, Y.-C.; Wickenburg, S.; Riss, A.; Mowbray, D. J.; Etkin, G.; Pedramrazi, Z.; Tsai, H.-Z.; Rubio, A.; Crommie, M. F.; Fischer, F. R. *Science* **2013**, *340*, 1434−1437.

(24) Kataura, H.; Maniwa, Y.; Abe, M.; Fujiwara, A.; Kodama, T.; Kikuchi, K.; Imahori, H.; Misaki, Y.; Suzuki, S.; Achiba, Y. *Appl. Phys. A: Mater. Sci. Process.* **2002**, *74*, 349−354.

(25) Solin, N.; Koshino, M.; Tanaka, T.; Takenaga, S.; Kataura, H.; Isobe, H.; Nakamura, E. *Chem. Lett.* **2007**, *36*, 1208−1209.

(26) *MacroModel*, version 9.7; Schrödinger, LLC: New York, NY, 2009.

(27) *Materials Studio*, version 5.0; Accelrys Software Inc.: San Diego, CA, 2009.

(28) Kirkland, E. J. *Advanced Computing in Electron Microscopy*; Plenum: New York, 1998.